Published in final edited form as:
Int J Parasitol. 2006 April ; 36(4): 433–441. doi:10.1016/j.ijpara.2006.01.006.

Proliferation of *Toxoplasma gondii* in inflammatory macrophages in vivo is associated with diminished oxygen radical production in the host cell

Sunder P. Shrestha[a], **Tadakimi Tomita**[a], **Louis M. Weiss**[a,b], and **Amos Orlofsky**[a,*]

[a]Department of Pathology, Albert Einstein College of Medicine, 1300 Morris Park Avenue, G704, Bronx, NY 10461, USA

[b]Division of Infectious Diseases, Department of Medicine, Albert Einstein College of Medicine, 1300 Marris Park Avenue, G704 Bronx, NY 10461, USA

Abstract

While reactive oxygen species (ROS) can kill *Toxoplasma gondii* in vitro the role these molecules play in vivo is not known. We used a flow cytometry-based assay to investigate the relationship between intracellular infection and ROS production during acute peritoneal toxoplasmosis in mice. A distinct population of ROS^+ inflammatory macrophages, detected by the oxidation of hydroethidine, was observed to increase progressively in frequency during the course of infection, and to be inversely correlated with the degree of cell parasitization. These data imply that either intracellular parasites inhibit ROS synthesis or, alternatively, ROS-producing cells contain anti-*Toxoplasma* activity. The latter interpretation was supported by the finding that uninfected ROS-producing inflammatory macrophages were resistant to infection in vivo. However, in the same animals, ROS-producing macrophages that had previously been parasitized could readily be infected with additional parasites, suggesting that the difference in ROS production between highly infected and less infected cells was not due to ROS-associated killing of parasites within these cells. In addition, macrophages infected with *T. gondii* in vitro and then briefly transferred to acutely infected mice upregulated ROS production in a manner that was again inversely correlated with the degree of intracellular parasitization. Taken together, these findings suggest that both ROS-associated anti-*Toxoplasma* activity and parasite-driven inhibition of ROS production underlie the observed pattern of ROS production. ROS function and parasite evasion of this function may contribute significantly to the balance between host defense and disease progression during acute infection.

Keywords

Toxoplasma gondii; Reactive oxygen species; Mice; Inflammation; Macrophages

1. Introduction

A critical aspect of host defense to *Toxoplasma gondii* is the activation of parasiticidal mechanisms in host leukocytes. Studies using mouse models of toxoplasmosis have suggested roles for several anti-parasite functions, including tryptophan catabolism and nitric oxide production, as well as uncharacterized functions mediated by members of the p47 GTPase family (Collazo et al., 2001; Pfefferkorn et al., 1986; Scharton-Kersten et al.,

*Corresponding author. Tel.: +718 430 2674; fax: +718 430 8867. orlofsky@aecom.yu.edu (A. Orlofsky).

1997). On the other hand, although reactive oxygen species (ROS) can mediate parasite killing in cell culture models (Aline et al., 2002; Murray et al., 1985), this mechanism appears to be inessential in vivo (Alexander et al., 1997), and ROS production is not triggered by parasite invasion of cultured macrophages (Wilson et al., 1980). The effect of ROS in vivo might be obscured by the presence of additional antiparasitic functions; alternatively the parasite may possess effective defenses against ROS, as indicated by its expression of antioxidant enzymes (Brydges and Carruthers, 2003; Kwok et al., 2004). Thus the involvement of this arm of host defense, a critical element of the response to many pathogens, remains undefined for *T. gondii*.

In mice acutely infected with a virulent strain of *T. gondii*, the inflammatory macrophage serves as a major reservoir for the parasite (Orlofsky et al., 1999). While macrophage respiratory burst is a well-studied in vitro phenomenon, few studies have examined this functionality in situ in response to infection. We undertook to directly examine ROS production in *T. gondii*-elicited inflammatory cells and assess the relationship of this production to intracellular infection and proliferation of the pathogen. Our results suggest that parasite proliferation in vivo is dependent on the absence or suppression of the respiratory burst, and that the role of ROS in host defense to *T. gondii* is deserving of further investigation.

2. Materials and methods

2.1. Infection of mice and analysis of parasitization

Mice (female C57BL/6, 6–8 weeks old) were obtained from The Jackson Laboratory. Mice were infected i.p. with 2000 tachyzoites of the RH strain (Type I) of *T. gondii* in PBS. The maintenance of *T. gondii* has been previously described (Weiss et al., 1995). Some experiments employed modified RH strains that express either yellow fluorescent protein (YFP) behind a tubulin promoter (kind gift of Dr B. Striepen, Univ. Georgia) (Gubbels et al., 2003) or green fluorescent protein (GFP) behind a GRA1 promoter (Ma et al., 2004). For superinfection of YFP-RH-infected mice with GFP-RH, mice infected 5–6 days earlier with YFP-RH were injected i.p. with 1.5×10^6 washed GFP-RH tachyzoites in 0.15 ml PBS. Pilot experiments with cultured macrophages infected with GFP-RH, YFP-RH or both were conducted to establish gating parameters to discriminate these strains. Discrimination was achieved in a LSRII cyotmeter (Becton Dickinson, San Jose, CA) by simultaneous acquisition of 488 nm-excited emissions collected with filter sets for either GFP (510 ± 20 +505 nm longpass) or YFP (550 ± 30 +530 nm longpass). All studies were conducted prior to the onset of morbidity at day 7 post-infection and were approved by the Albert Einstein College of Medicine animal care and use committee.

2.2. Assay of oxygen radical formation

Mice were sacrificed by cervical dislocation following isoflurane anaesthesia. The peritoneal cavity was lavaged with ice-cold Hank's solution + 1% FCS (HyClone, Logan, UT). The cell suspension was washed and resuspended in this buffer at approximately 5×10^6 cells/ml, and then incubated with 10 μM hydroethidine (HE; Molecular Probes, Eugene, OR) for 30 min at 37 °C. The suspension was then placed on ice, incubated with Fc-Block + Alexa647-conjugated anti-CD11b or Alexa647-anti-F4/80 (Becton Dickinson) and analyzed by flow cytometry on a FACS Calibur (Becton Dickinson). Assessment of propidium iodide staining was performed on separate samples (not stained with HE) to confirm that the proportion of inviable macrophages was small relative to the HE-positive population.

2.3. Morphological assessment of cell populations

Peritoneal lavage was obtained from mice infected 5 days earlier with YFP-RH, stained with Alexa647-anti-F4/80 and fixed with 4% paraformaldehyde. Cells were sorted on a MoFlo sorter (Dako, Fort Collins, CO) and the resulting fractions were cytocentrifuged and stained with Hoechst33342 to define nuclear morphology. At least 200 cells were scored to determine the proportion of mononuclear cells.

2.4. Macrophage transfer

Peritoneal exudate macrophages (PEM) were obtained by peritoneal lavage of mice 5 days after injection of 1 ml of 3% thioglycollate broth (Difco). Pooled PEM from five mice were suspended in RPMI medium containing 10% FCS + 10% DMSO at 10×10^6/ml and aliquots were frozen. For each experiment an aliquot was thawed two days prior to transfer and cultured in RPMI + 10% FCS (5×10^5 cells/ml) in non-adherent vessels (Corning Life Sciences, Acton, MA). One day before transfer, cultures were infected with YFP-RH tachyzoites at m.o.i. = 1, thus yielding a mixture of infected and uninfected cells. Immediately before transfer, PEM were labeled by the addition of 10 uM BODIPY methyl bromide 630/650 (Molecular Probes) for 30 min. The cells were then centrifuged, washed twice with cold PBS, suspended in cold PBS at 5×10^6/ml, warmed for 2 min at 37 °C, and injected i.p. (0.1 ml) into mice infected 5 days previously. Peritoneal lavage fluid was taken at 90 min after transfer and analyzed as above, except that marker antibodies were not employed as only the recovered donor macrophages were analyzed. In these experiments the infection of host mice was carried out with non-fluorescent RH, so that donor cells would not be falsely scored as infected due to their engulfment of infected host neutrophils after transfer.

2.5. Statistical methods

Statistical significance of the difference in ROS formation between cell populations was assessed using Student's *t*-test For paired *t*-tests, cell populations were paired with populations of different infection status obtained from the same animal. This approach minimizes the impact of global variation in ROS formation among individual mice. The linearity of the relationship between parasite fluorescence and parasite number per cell was assessed with Pearson's correlation coefficient (r^2). Statistical analysis was performed using Sigma Plot 8.0 (SPSS, Chicago, IL).

3. Results

3.1. Progressive accumulation of ROS during acute infection

Intraperitoneal infection of mice with the RH strain of *T. gondii* generates a severe acute inflammatory reaction characterized by massive peritoneal leukocytosis that in our experiments begins at day 3 to day 4 post-infection and continues until the host is overwhelmed by the parasite at day 7–8. We and others have previously shown that macrophages and neutrophils are major components of the inflammatory exudate in this model, and that the macrophage is a major host cell for the parasite within this exudate (Mordue and Sibley, 2003; Orlofsky et al., 1999).

There are few studies describing ROS production in macrophages during acute inflammation. Since the initial step in ROS production is the generation of superoxide anion by reduced nicotinamide adenine dinucleotide phosphate (NADPH) oxidase, we decided to employ an assay that could detect this radical at the single-cell level. We chose to use hydroethidine (HE), which is converted to a red-fluorescent product in the presence of superoxide and is widely used as an intracellular indicator for this species, although other oxygen radicals can also generate products with HE (Zhao et al., 2003).

Flow cytometric analysis of the inflammatory exudate identified a population of presumptive macrophages as large (high forward scatter) CD11b$^+$ cells (Fig. 1A). We chose CD11b as a marker for initial studies to ensure that all cells of the monocyte/macrophage series were included. Since this method does not entirely exclude neutrophils, we refer to this populations as 'myeloid inflammatory cells'. Staining of this population with HE produced a clear bimodal distribution at day 5 post-infection (Fig. 1B), indicating oxygen radical formation in a subset of myeloid inflammatory cells. We denote this subset as ROS$^+$, and the HE-dim myeloid subset as ROS$^-$. The mean fluorescent intensity of ROS$^+$ was 7.2 ± 0.8 times the intensity of ROS$^-$ (n = 4). The ROS$^+$ fraction of myeloid inflammatory cells showed a progressive elevation during the course of infection, increasing from a basal level of approximately 10% to approximately 40% by day 5 (Fig. 2). This progression is a consistent finding; however the absolute level of ROS$^+$ shows variation among animals and among experiments. In six experiments (combined n = 19), the ROS$^+$ fraction in myeloid inflammatory cells at day 5 had a mean value of 18 ± 3%.

3.2. ROS levels inversely correlate with degree of intracellular parasitization

As shown in Fig. 1B, the use of the YFP-RH parasite strain permitted clear discrimination of infected and uninfected myeloid inflammatory cells, and by day 5 post-infection the ROS$^+$ fraction of infected cells was 32 ± 3% less than that of the uninfected population (Fig. 2). To examine the relationship between the degree of intracellular parasitization and ROS levels, we assessed intracellular parasite content by YFP intensity. As shown in Fig. 3, YFP intensity was distributed in discrete populations, for each of which a peak value could be calculated. These peaks represent cells infected with 1–3, and ≥ 4 parasites/cell, as shown by the excellent agreement of observed and predicted peak intensities (Fig. 3B), as well as the agreement of peak-1 intensity with the intensity of extracellular single tachyzoites (not shown). In mice from three independent experiments, the square of the correlation coefficient of peak intensity with peak number was 0.998 ± 0.008, indicating a strongly linear relationship. The regression coefficient was 0.855 ± 0.04. This value is slightly less than the predicted value of 1, most likely reflecting self-absorption of emission within the parasitophorous vacuole.

This method of parasite enumeration revealed a clear inverse relationship between intracellular parasite content and the fraction of ROS$^+$ (Fig. 4). Cells containing at least four parasites had a ROS$^+$ fraction about five-fold reduced compared to uninfected myeloid cells, while minimally infected cells showed only a modest, although statistically significant, reduction. The ROS$^+$ fraction in these highly infected cells was not different from the fraction observed in peritoneal macrophages in control uninfected mice (compare Fig. 4B with Fig. 2).

3.3. Parasite-associated ROS deficit is most prominent in large, highly infected macrophages

To examine further the cell types in which infection was associated with a low ROS$^+$ fraction, we conducted a similar analysis with inflammatory cells stained for the macrophage maker F4/80. We chose this marker for the discrimination of myeloid cell subtypes, rather than the granulocytic marker Gr-1, because the latter antigen is expressed on macrophages in this system (Mordue and Sibley, 2003, and our unpublished observations). Mordue and Sibley also found that F4/80 is less intensely expressed on *T. gondii*-elicited macrophages, compared to other macrophage populations. We therefore first verified the effectiveness of F4/80 in identifying a mononuclear population free of granulocytes. As shown in Fig. 5, a distinct F4/80$^+$ population was readily identified, and microscopic analysis of sorted F4/80$^+$ cells demonstrated their mononuclear morphology.

By differential counting, this population was 95% mononuclear, whereas the F4/80$^-$ population was 30% mononuclear.

When F4/80$^+$ cells were examined for ROS, an inverse correlation of ROS$^+$ fraction with degree of intracellular parasitization was once again observed (Fig. 6C). In contrast, the F4/80$^-$ population had only a small number of ROS$^+$ cells (<1%) that demonstrated no correlation with intracellular parasite content (data not shown). Therefore the parasite-associated ROS deficit is a feature of inflammatory macrophages.

The F4/80$^+$ population displays a broad distribution with respect to forward scatter (Fig. 6B). We examined whether the parasite-associated ROS deficit was concentrated in a particular region of this spectrum. We divided the F4/80$^+$ cells into two fractions, above and below the geometric mean of the forward scatter distribution. The 'large macrophage' subset defined in this way is about 40% of the total F4/80$^+$ population. As shown in Fig. 6D–E, the reduction in ROS$^+$ fraction in lightly infected F4/80$^+$ cells (<4 parasites/cell), compared to uninfected cells, was similar for the large and small macrophage subsets, although it is more pronounced in the large subset. However when highly infected macrophages were compared to the lightly infected cells, large cells displayed a severe reduction in ROS$^+$ fraction (Fig. 6D), similar to that observed previously for large CD11b$^+$ cells (Fig. 4). Small F4/80$^+$ cells did not show a comparable reduction, and in the experiment shown the ROS$^+$ fraction actually increased in highly infected small cells (Fig. 6E). This increase is a variable finding; however large macrophages consistently show a more pronounced reduction in ROS$^+$ as a function of increased parasitization than do small F4/80$^+$ cells. We considered the possiblity that the results might reflect a greater number of parasites/cell in the highly infected large compared to highly infected small populations. However when we restricted the analysis of highly infected cells to a window of 4–5 parasites/cell, identical data were obtained (Fig. 6F). Therefore the parasite-associated ROS deficit is a feature of large, highly infected inflammatory macrophages.

In view of the higher frequency of ROS$^+$ in highly infected small F4/80$^+$ cells, we asked whether the small F4/80$^+$ cell population was less infected overall compared to larger macrophages. Indeed the frequency of infection in small cells was 50% (± 1.5%) compared to 72% (± 1.7%) in large cells (n = 5). Furthermore, among the infected cells the mean number of parasites/cell was 1.9 (± 0.05) for small cells compared to 3.4 (± 0.06) for large cells.

3.4. ROS$^+$ cells that are free of parasites are resistant to infection in vivo

We next sought to investigate the basis for the inverse correlation of ROS and intracellular parasites. One possibility is that *Toxoplasma* actively suppresses ROS generation in mature macrophages. Alternatively, ROS$^+$ macrophages possess an anti-*Toxoplasma* activity and thus fail to support either the invasion, survival, proliferation and/or retention of parasites. To examine the possibility of anti-*Toxoplasma* activity in ROS$^+$ macrophages, we asked whether these cells were susceptible to invasion by tachyzoites in situ. Mice that had been infected 5 days earlier with YFP-RH were infected with 1.5×10^6 GFP-RH tachyzoites, followed by lavage and HE—positive anti-F4/80 staining 1 h later. Large and small cells were not discriminated in this experiment. The total number of extracellular YFP-RH in the peritoneal cavity in these mice was approximately 4×10^6 (data not shown), so the GFP-RH inoculum represents a modest increase in the total extracellular parasite content, and a negligible increase in total mouse burden, since the great majority of the parasites (>80%) are intracellular (data not shown). By the time the peritoneal cavity is lavaged, 97% of the recoverable GFP-RH tachyzoites are cell-associated (data not shown). As shown in Fig. 7A, GFP-RH and YFP-RH are sufficiently distinguishable by flow cytometry to permit clear identification of cells that simultaneously harbor both strains, as well as each strain individually. Therefore it is possible to separately assess the suseptibility to GFP-RH infection of macrophages that either were or were not already infected with YFP-RH prior to GFP-RH injection. In each case, the question was whether ROS status would affect susceptibility.

As shown in Fig. 7B, F4/80$^+$ macrophages that already harbored YFP-RH parasites ('previously infected Mϕ'), were equivalently susceptible to GFP-RH infection regardless of ROS status. In contrast, macrophages devoid of YFP-RH were susceptible if they were ROS$^-$ but highly resistant if they were ROS$^+$. The frequency of successful GFP-RH invasion of ROS$^+$ YFP-null macrophages was less than that of ROS$^-$ YFP-null cells by 87 ± 26-fold (mean ± SE, n = 6).

3.5. Short-term exposure to the ROS-inducing microenvironment is sufficient to generate a parasite-associated ROS deficit

The results of Fig. 7 suggest the existence of an anti-*Toxoplasma* activity in ROS$^+$ uninfected macrophages. This activity might be a sufficient explanation for the reduced ROS$^+$ fraction observed in the total population of infected compared to uninfected macrophages. That is, if parasites preferentially infect ROS$^-$ uninfected macrophages that are potentially less prone to activation of oxidative burst, infected cells will be less likely to be ROS$^+$. However it is still necessary to account for the more specific and pronounced ROS deficit in highly infected large macrophages, compared to less infected cells, and in this case the data from Fig. 7 suggest that toxoplasmacidal activity is not the cause, since ROS$^+$ infected cells are permissive to *Toxoplasma*, at least to the extent that short-term superinfection is not impeded.

One possible explanation is that ROS$^+$ cells do not support parasite proliferation and lightly-infected ROS$^+$ cells thus fail to progress to a highly-infected stage. Alternatively, high levels of intracellular parasitization might inhibit ROS production. To help distinguish between these possibilities, we asked to what extent de novo generation of ROS can be detected in macrophages that already harbor various numbers of parasites. For this purpose, thioglycollate-elicted macrophages were infected with YFP-RH (yielding a mixture of infected and uninfected cells), allowed to progress overnight in an environment that does not induce ROS (cell culture medium), and only then briefly exposed to a ROS-inducing inflammatory microenvironment by transfer for 90 min to the peritoneal cavity of mice infected 5 days earlier with non-fluorescent RH. The recovered cells (labeled with a vital dye) were then HE-stained to determine whether their parasitization status affected their development of ROS in vivo. If the ROS deficit were simply the result of a ROS-mediated block in proliferation, then the predicted result is uniform ROS production (since proliferation has now been separated from ROS induction), whereas a suppressive mechanism would predict the opposite.

Prior to transfer the donor cells displayed a single population of HE-stained cells (Fig. 8A). After transfer, recovered donor macrophages showed a bimodal distribution of staining indicative of ROS induction in vivo (Fig. 8C and D). The recovered cells displayed a parasite-associated ROS deficit comparable to that previously observed for endogenous host cells. This was the case both with respect to the total population of infected cells, compared to uninfected cells (Fig. 8E, left panel), and also with respect to the degree of infection of the infected cells (Fig. 8E, right panel). Due to the limited number of analyzable cells, we compared cells harboring one parasite to those with >1 parasite, rather than <4 and ≥4 as in previous experiments. Cells with >1 parasite had a ROS$^+$ fraction 31% less than those with one parasite.

NIH-PA Author Manuscript

NIH-PA Author Manuscript

4. Discussion

The results reported here provide the first in vivo evidence that the oxidative state of the inflammatory macrophage, the major host cell for *T. gondii* in a mouse model of acute infection, is a matter of consequence for the parasite. We draw this inference from two findings. First, in large macrophages, extensive parasite proliferation (two or more rounds of division) is strongly biased to ROS^{-} cells. Second, uninfected ROS^{+} cells are resistant to infection in vivo. These findings are consistent with previous studies that indicate both toxoplasmastatic and toxoplasmacidal activity of ROS in cultured monocytes, macrophages and dendritic cells (Aline et al., 2002; Murray and Nathan, 1999). Therefore evasion of ROS may be a necessary component of parasite strategy for successful proliferation. However it is not likely to be sufficient in itself, since a variety of non-oxidative anti-parasite functions can also occur in these cells (Alexander et al., 1997). The co-existence of oxidative and non-oxidative mechanisms may account for the failure to find significant impairment of host defense in ROS-deficient mice (Alexander et al., 1997).

Two of our findings can be viewed as being at variance with the interpretation that *T. gondii* needs to evade ROS. First, small $F4/80^{+}$ cells can produce substantial levels of ROS even when multiply infected. However our data indicate that the parasite burden is considerably smaller in the small compared to the large macrophages, and so it is possible that the frequency of ROS^{+} among small $F4/80^{+}$ cells reflects successful anti-*Toxoplasma* activity in these cells. Second, ROS^{+} cells previously infected with *T. gondii* in situ are as susceptible to further infection as ROS^{-} cells. However we have not yet examined the ability of the parasite to successfully proliferate in these ROS^{+} cells.

A simple model that accommodates these findings is one that posits multiple levels of anti-*Toxoplasma* activation among macrophages. For example, a subset of inflammatory macrophages may become activated to generate both ROS-mediated and ROS-independent anti-*Toxoplasma* functions. These highly activated cells (which we observe as ROS^{+} uninfected $F4/80^{+}$ cells) destroy parasites either during or shortly after invasion and are therefore resistant to infection. A second population of macrophages becomes infected before such activation takes place. It is to be expected that these infected cells will rapidly become partially inhibited with respect to the generation of nitric oxide, an important non-ROS anti-*Toxoplasma* agent (Dobbin et al., 2002; Lüder et al., 2003; Seabra et al., 2002). However, according to our results, these cells can still produce ROS to some extent, and ROS production in these cells may mediate a more limited toxoplasmastatic or toxoplasmacidal activity that does not prevent short-term (1 h) infection. Finally, a subset of this population are large macrophages in which the ROS activation mechanism is absent or suppressed, and these cells provide a safe haven for the parasite in which substantial proliferation can take place. Whether these large infected macrophages are derived from smaller infected cells is not yet determined.

A notable aspect of our results is the clear demonstration of a subset of inflammatory cells (the ROS^{+} uninfected macrophages) that are distinctly resistant to infection in situ. The reduction in susceptibility in these cells compared to their ROS^{-} counterparts is nearly two orders of magnitude. In view of this finding, it will be important to understand the nature of the signals that give rise to the resistant population, the consequences of these signals for macrophage activation, and whether this activation is transient and stochastically distributed among all uninfected macrophages or alternatively a stable property of a distinct macrophage subtype.

It remains uncertain from our results whether *T. gondii* can actively suppress ROS in macrophages. Our finding that transferred macrophages rapidly acquire a ROS pattern inversely correlated with intracellular parasitization is suggestive of a suppressive mechanism. A caveat to this experiment is that a portion of the observed ROS deficit in transferred cells could have been produced by a ROS-mediated blockade of proliferation during the 90 min transfer period. Assuming a parasite replication cycle of 6 h, 25% of the cells in the one parasite/cell fraction might have entered the >1 parasite/cell population during transfer. Assuming this occurred, based on the size of the ‘one parasite/cell’ subset in the donor population prior to transfer, the predicted mean ROS deficit from proliferative blockade alone is 23%, less than the 31% observed. Moreover this calculation assumes immediate induction of ROS upon transfer and complete and immediate inhibition of parasite proliferation in ROS^+ cells. Therefore while such inhibition might account for some of the ROS deficit, blockade of parasite proliferation is unlikely to be sole mechanism generating the pattern of ROS production we have observed.

While we favor the interpretation of the cell transfer data as supportive of a suppressive mechanism, the results can also be explained in other ways. It is possible that ROS induction in transferred cells rapidly induces parasite death or egress, or that highly infected ROS^+ transferred cells are sequestered or killed in vivo. In support of a suppressive mechanism are studies demonstrating a number of antioxidant activities in *T. gondii* (Brydges and Carruthers, 2003; Kwok et al., 2004), of which at least one catalase has been implicated in pathogenesis by genetic evidence (Kwok et al., 2004). These activities include superoxide dismutases that might degrade superoxide and prevent HE oxidation. However these parasite-encoded functions are likely to operate within the tachyzoite, and therefore it is not clear that they would suffice to prevent HE oxidation by superoxide generated at the parasitophorous vacuole membrane or other locations within the host cell. Alternatively, *T. gondii* may actively suppress the activation of NADPH oxidase in macrophages, and thus prevent the generation of superoxide. We have not observed such inhibition in the case of the phorbol ester-triggered burst in cultured peritoneal exudate macrophages (unpublished observations), and a previous study found no inhibition by *T. gondii* of the burst stimulated by *Candida albicans* (although this study examined only brief infection by *Toxoplasma*) (Wilson et al., 1980). However many signaling mechanisms govern oxidase activation in phagocytes, and it is possible that the (unidentified) signals responsible for macrophage superoxide production in vivo are susceptible to inhibition by the parasite. For example, ROS production in *T. gondii*-infected cultured macrophages requires priming by IFNγ (Murray et al., 1985), and the parasitization of the cell may inhibit the priming signal.

Although in vivo studies have repeatedly indicated a role for ROS in the early containment of both bacterial and parasitic pathogens (Murray and Nathan, 1999; Nathan and Shiloh, 2000), few have demonstrated activated ROS production in inflammatory macrophages during acute infection. Our findings point to novel approaches to investigating the regulation and function of ROS in vivo, and suggest that in the case of *Toxoplasma*, evasion of ROS may be an important step in pathogenesis. The nature of this evasion, as well as the mechanism of activation of ROS production in vivo, present subjects for future experiments.

Acknowledgments

We gratefully acknowledge the technical assistance of Yanfen Ma. We thank William King (AECOM FACS Core Facility) for his assistance with cell sorting. This study was supported by funds from National Institutes of Health grant AI-55358 to A.O and AI-39454 to L.M.W., and by the Flow Cytometry Core of the Center for AIDS Research (AI-51519).

References

Alexander J, Scharton-Kersten TM, Yap G, Roberts CW, Liew FY, Sher A. Mechanisms of innate resistance to *Toxoplasma gondii* infection. Philos. Trans. R. Soc. Lond. B Biol. Sci. 1997; 352:1355–1359. [PubMed: 9355127]

Aline F, Bout D, Dimier-Poisson I. Dendritic cells as effector cells: gamma interferon activation of murine dendritic cells triggers oxygen-dependent inhibition of *Toxoplasma gondii* replication. Infect. Immun. 2002; 70:2368–2374. [PubMed: 11953372]

Brydges SD, Carruthers VB. Mutation of an unusual mitochondrial targeting sequence of SODB2 produces multiple targeting fates in *Toxoplasma gondii*. J. Cell Sci. 2003; 116:4675–4685. [PubMed: 14576360]

Collazo CM, Yap GS, Sempowski GD, Lusby KC, Tessarollo L, Woude GF, Sher A, Taylor GA. Inactivation of LRG-47 and IRG-47 reveals a family of interferon gamma-inducible genes with essential, pathogen-specific roles in resistance to infection. J. Exp. Med. 2001; 194:181–188. [PubMed: 11457893]

Dobbin CA, Smith NC, Johnson AM. Heat shock protein 70 is a potential virulence factor in murine toxoplasma infection via immuno-modulation of host NF-kappa B and nitric oxide. J. Immunol. 2002; 169:958–965. [PubMed: 12097402]

Gubbels M-J, Li C, Striepen B. High-throughput growth assay for *Toxoplasma gondii* using yellow fluorescent protein. Antimicrob. Agents Chemother. 2003; 47:309–316. [PubMed: 12499207]

Kwok LY, Schluter D, Clayton C, Soldati D. The antioxidant systems in *Toxoplasma gondii* and the role of cytosolic catalase in defence against oxidative injury. Mol. Microbiol. 2004; 51:47–61. [PubMed: 14651610]

Lüder CG, Algner M, Lang C, Bleicher N, Gross U. Reduced expression of the inducible nitric oxide synthase after infection with *Toxoplasma gondii* facilitates parasite replication in activated murine macrophages. Int. J. Parasitol. 2003; 33:833–844. [PubMed: 12865083]

Ma YF, Zhang Y, Kim K, Weiss LM. Identification and characterisation of a regulatory region in the Toxoplasma gondii hsp70 genomic locus. Int. J. Parasitol. 2004; 34:333–346. [PubMed: 15003494]

Mordue DG, Sibley LD. A novel population of Gr-1+-activated macrophages induced during acute toxoplasmosis. J. Leukoc. Biol. 2003; 74:1015–1025. [PubMed: 12972511]

Murray HW, Nathan CF. Macrophage microbicidal mechanisms in vivo: reactive nitrogen versus oxygen intermediates in the killing of intracellular visceral Leishmania donovani. J. Exp. Med. 1999; 189:741–746. [PubMed: 9989990]

Murray HW, Rubin BY, Carriero SM, Harris AM, Jaffee EA. Human mononuclear phagocyte antiprotozoal mechanisms: oxygen-dependent vs oxygen-independent activity against intracellular *Toxoplasma gondii*. J. Immunol. 1985; 134:1982–1988. [PubMed: 2981929]

Nathan C, Shiloh MU. Reactive oxygen and nitrogen intermediates in the relationship between mammalian hosts and microbial pathogens. Proc. Natl Acad. Sci. USA. 2000; 97:8841–8848. [PubMed: 10922044]

Orlofsky A, Somogyi RD, Weiss LM, Prystowsky MB. The murine antiapoptotic protein A1 is induced in inflammatory macrophages and constitutively expressed in neutrophils. J. Immunol. 1999; 163:412–419. [PubMed: 10384143]

Pfefferkorn ER, Eckel M, Rebhun S. Interferon-gamma suppresses the growth of Toxoplasma gondii in human fibroblasts through starvation for tryptophan. Mol. Biochem. Parasitol. 1986; 20:215–224. [PubMed: 3093859]

Scharton-Kersten TM, Yap G, Magram J, Sher A. Inducible nitric oxide is essential for host control of persistent but not acute infection with the intracellular pathogen *Toxoplasma gondii*. J. Exp. Med. 1997; 185:1261–1273. [PubMed: 9104813]

Seabra SH, de Souza W, DaMatta RA. *Toxoplasma gondii* inhibits nitric oxide production by activated mouse macrophages. Exp. Parasitol. 2002; 100:62–70. [PubMed: 11971655]

Weiss LM, Laplace D, Takvorian PM, Tanowitz HB, Cali A, Wittner M. A cell culture system for study of the development of *Toxoplasma gondii* bradyzoites. J. Eukaryot. Microbiol. 1995; 42:150–157. [PubMed: 7757057]

Wilson CB, Tsai V, Remington JS. Failure to trigger the oxidative metabolic burst by normal macrophages: possible mechanism for survival of intracellular pathogens. J. Exp. Med. 1980; 151:328–346. [PubMed: 7356726]

Zhao H, Kalivendi S, Zhang H, Joseph J, Nithipatikom K, Vasquez-Vivar J, Kalyanaraman B. Superoxide reacts with hydroethidine but forms a fluorescent product that is distinctly different from ethidium: potential implications in intracellular fluorescence detection of superoxide. Free Radic. Biol. Med. 2003; 34:1359–1368. [PubMed: 12757846]

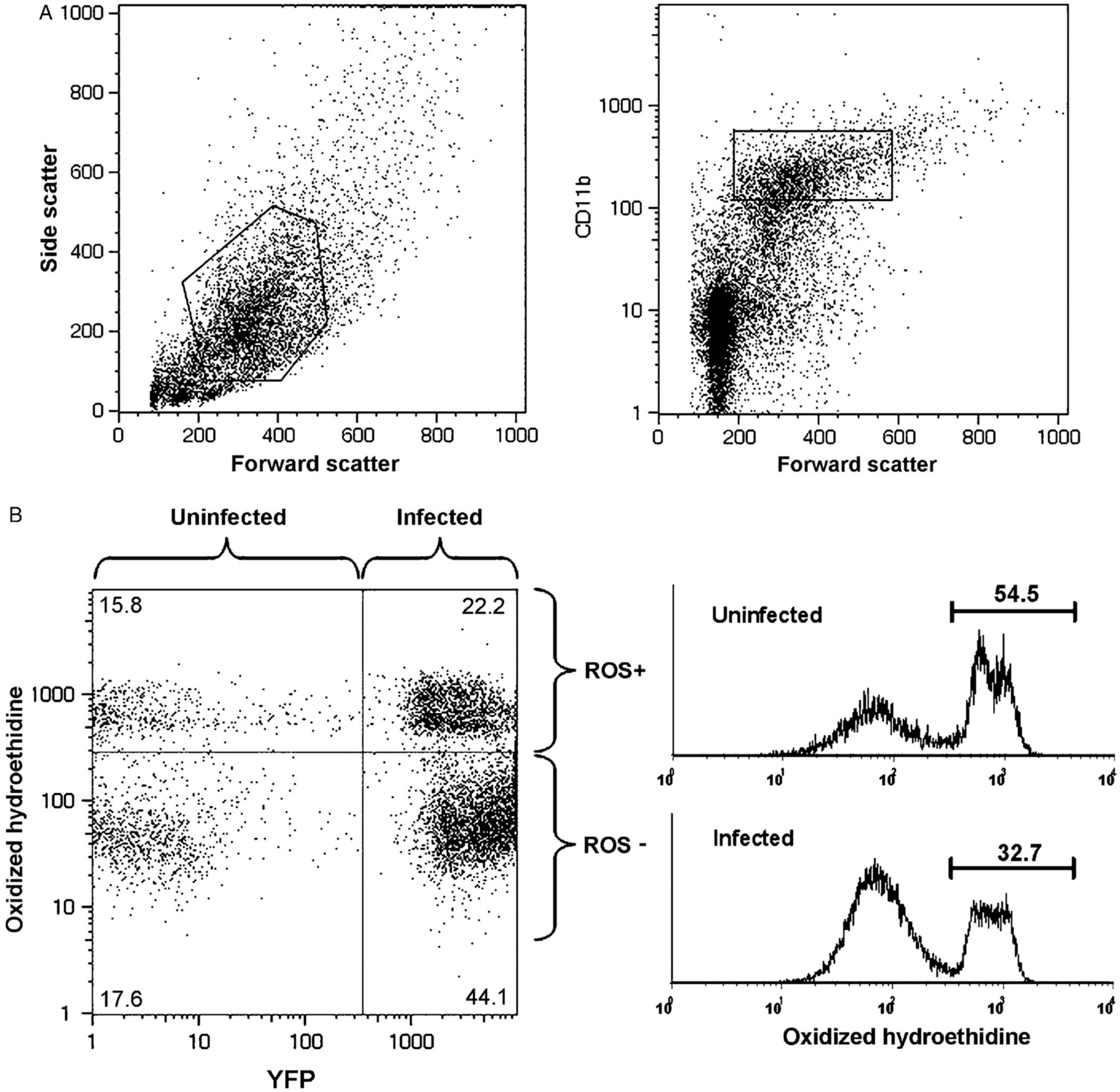

Fig. 1.

Acute infection results in elevated oxygen radical production in a subset of myeloid inflammatory cells. Exudate from mice infected with yellow fluorescent protein-expressing RH (YFP-RH) (d5 post-infection) was analyzed by flow cytometry. (A) A ‘myeloid inflammatory cell’ gate was defined by combining the indicated scatter gate (left panel) with a CD11b gate based on the intensity of surface CD11b staining (right panel). (B) Gated myeloid inflammatory cells were assessed for parasitization (YFP) and oxygen radical production (oxidized hydroethidine). Histograms (right panel) were used to measure fractions containing high or low levels of reactive oxygen species (ROS^+ and ROS^-, respectively). The numbers in panel B represent the percentages of gated cells contained within the indicated quadrant or region. The data are representative of four similar experiments.

NIH-PA Author Manuscript
NIH-PA Author Manuscript

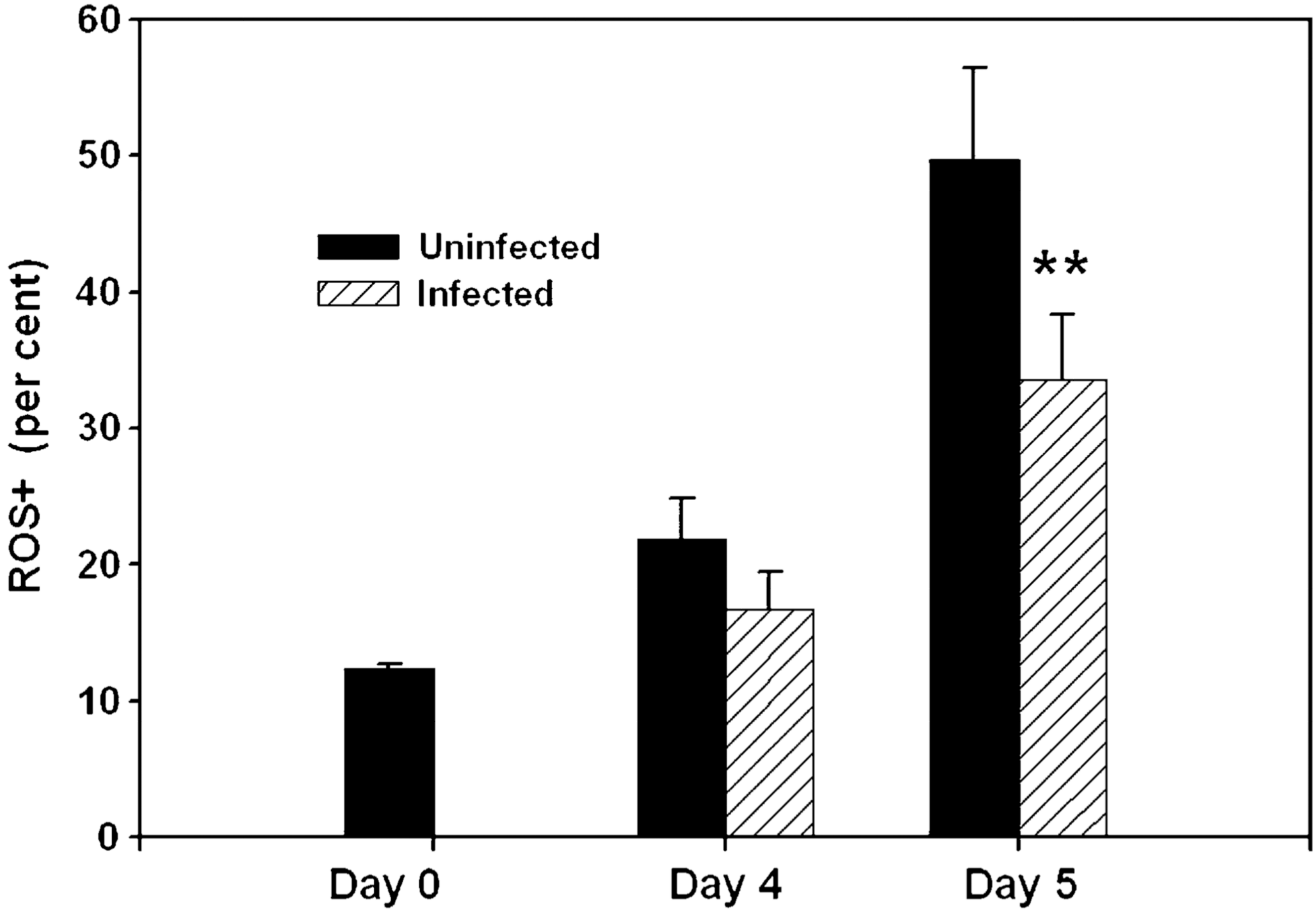

Fig. 2.

Parasitized myeloid inflammatory cells have reduced oxygen radical production in vivo. The percentage of myeloid inflammatory cells in the ROS^+ gate was assessed in acutely infected mice at the indicated times post-infection. Each bar represents the mean ± SEM of four mice. ***P* < 0.01 by paired *t*-test compared with uninfected. The data are representative of four similar experiments.

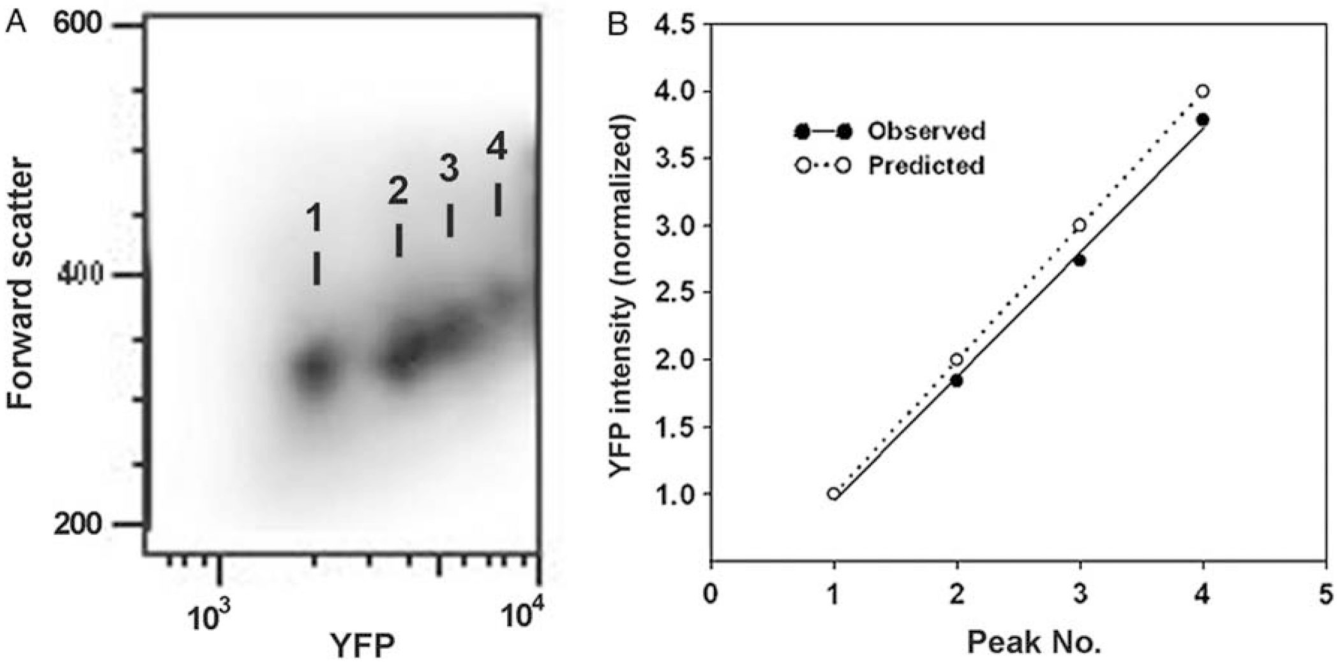

Fig. 3.
Enumeration of intracellular parasites by flow cytometry. Data represent gated myeloid inflammatory cells from exudates collected at day 5 post-infection. (A) Density plot showing peaks of YFP fluorescence. Numbers in (A) correspond to 'Peak Number' in panel (B). (B) YFP peak inensity values from panel (A) were normalized so that the intensity of peak 1 = 1. The observed values agree with the values predicted if the peaks represent successive increments of one parasite/cell.

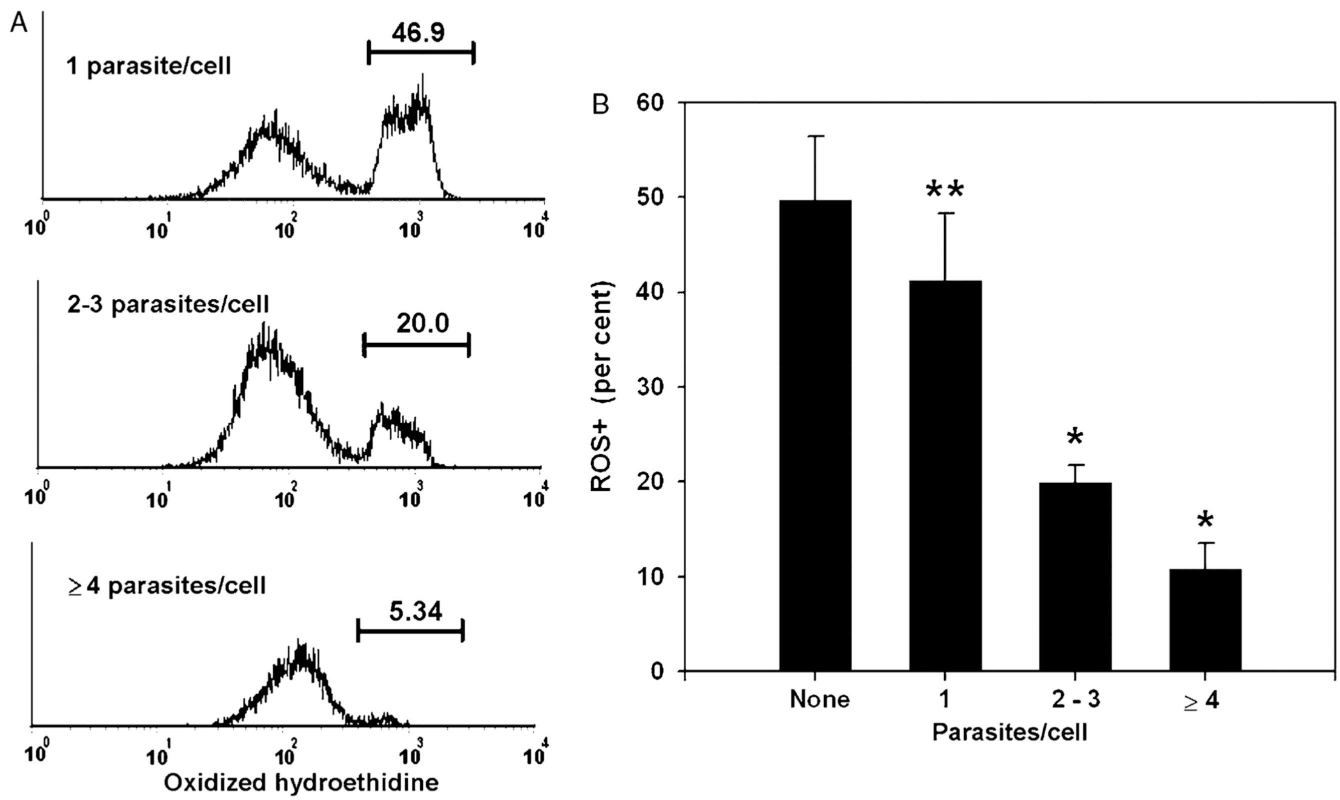

Fig. 4.

Inverse relationship between intracellular parasite content and oxygen radical production. Data represent gated myeloid inflammatory cells from exudates collected at day 5 post-infection. YFP-positive cells were assessed for intracellular parasite content as in Fig. 3 and divided into three gates, representing peak 1, peaks 2+3, and 'peak 4 or greater'. (A) ROS^+ fractions were determined for each gate by histogram analysis. Numbers represent the percentage of gated cells contained within the indicated ROS^+ region. The data in (B) represent mean ± SEM for four mice. ** $P < 0.001$ compared to uninfected cells by paired *t*-test. The low *p* value reflects the consistency of the difference between uninfected and infected cells when paired cell populations derived from the same animal are compared, while the error bars reflect, in addition, the variation in overall ROS^+ fraction among individual mice. * $P < 0.05$ compared to '1 parasite/cell' by paired *t*-test. Results are representative of three similar experiments.

NIH-PA Author Manuscript
NIH-PA Author Manuscript

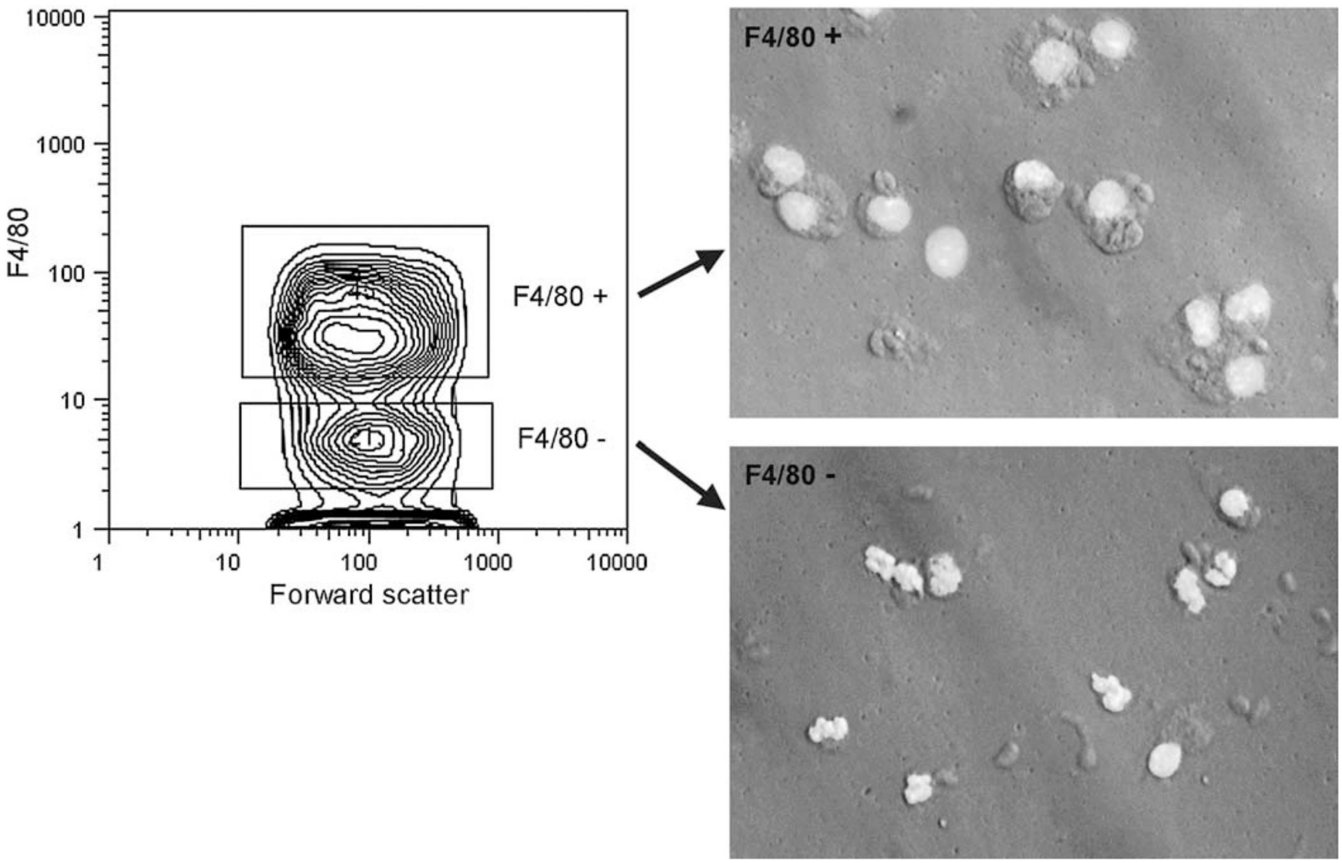

Fig. 5.

Morphology of F4/80+ inflammatory cells. Anti-F4/80-stained peritoneal exudate cells from infected mice (d5) were sorted, cytocentrifuged and stained with Hoechst 33342 for fluorescent micrography. Gates for sorting are indicated by a probability contour plot (left panel). Cells were simultaneously sorted with respect to presence or absence of parasite (not shown). Infected and uninfected fractions gave similar results. The micrographs shown are for infected fractions. Images of fluorescence and Hoffman interference contrast were obtained simultaneously.

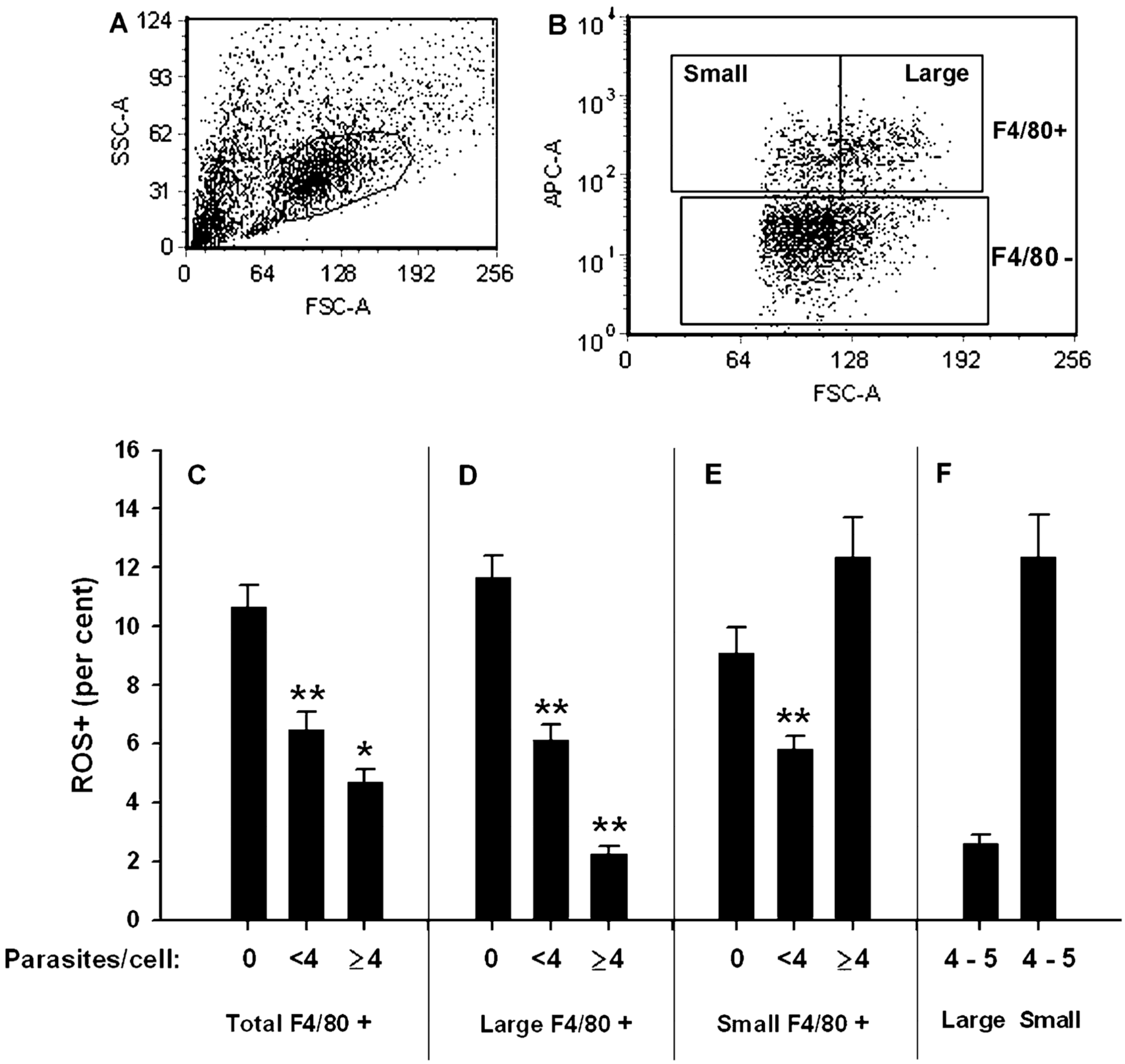

Fig. 6.

Relationship between parasite content and ROS in F4/80+ inflammatory cells. Exudate cells from infected mice (d6) were gated first for scatter (A) and then for F4/80 expression (ordinate in panel B) as well as size (abscissa in panel B). ROS^+ fractions were determined as for the previous experiments. Data represent mean ± SE for five mice and are representative of two similar experiments. * $P < 0.05$. ** $P < 0.01$. All P values represent comparison of either '<4 parasites' to 0 (asterisks placed over middle bar of the panel) or else '≥4' to '<4' (asterisks placed over right bar of the panel). For panel F, large and small F4/80+ cells of indentical parasite content (4–5 parasites/cell) were compared.

NIH-PA Author Manuscript
NIH-PA Author Manuscript

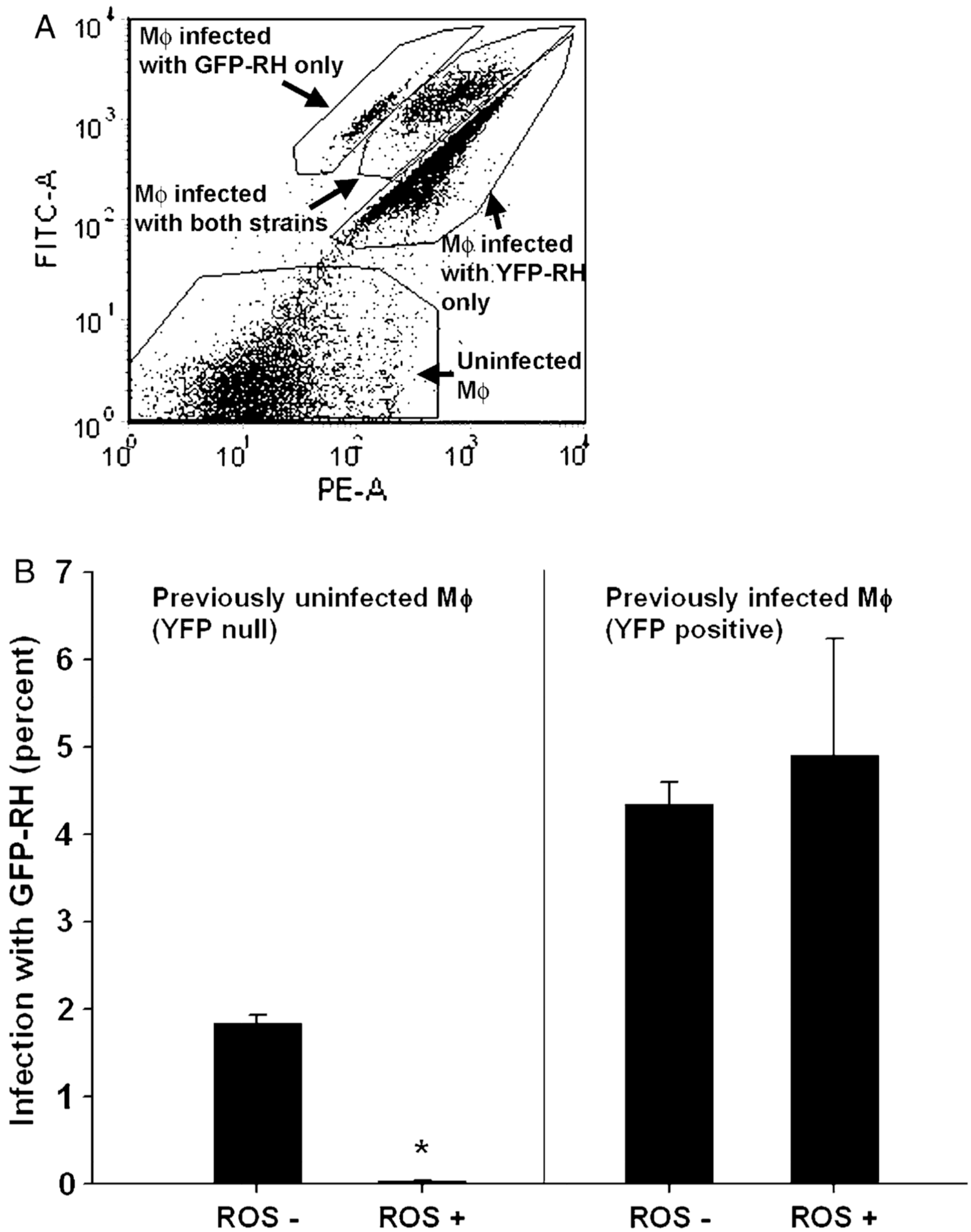

Fig. 7.

Susceptibility to infection in situ of inflammatory cells during acute toxoplasmosis. Mice infected 6 days earlier with YFP-RH were superinfected with green fluorescent protein-expressing RH (GFP-RH). Exudate cells were stained with anti-F4/80 and hydroethidine. For flow cytometry, all cells were gated for scatter and positive expression of F4/80 as in Fig. 6. Panel A shows the discrimination of GFP+ YFP−, GFP+ YFP+, GFP− YFP+ and GFP− YFP− cells. The ordinate represents signal acquired with the GFP filter set and the abscissa the YFP set. Cells were then further gated to distinguish ROS^+ and ROS^- fractions and the frequency of GFP-RH infection determined (B). The data represent mean ± SE from five mice. * $P = 0.00007$ compared to ROS^{-} by paired *t*-test. The data are representative of two similar experiments.

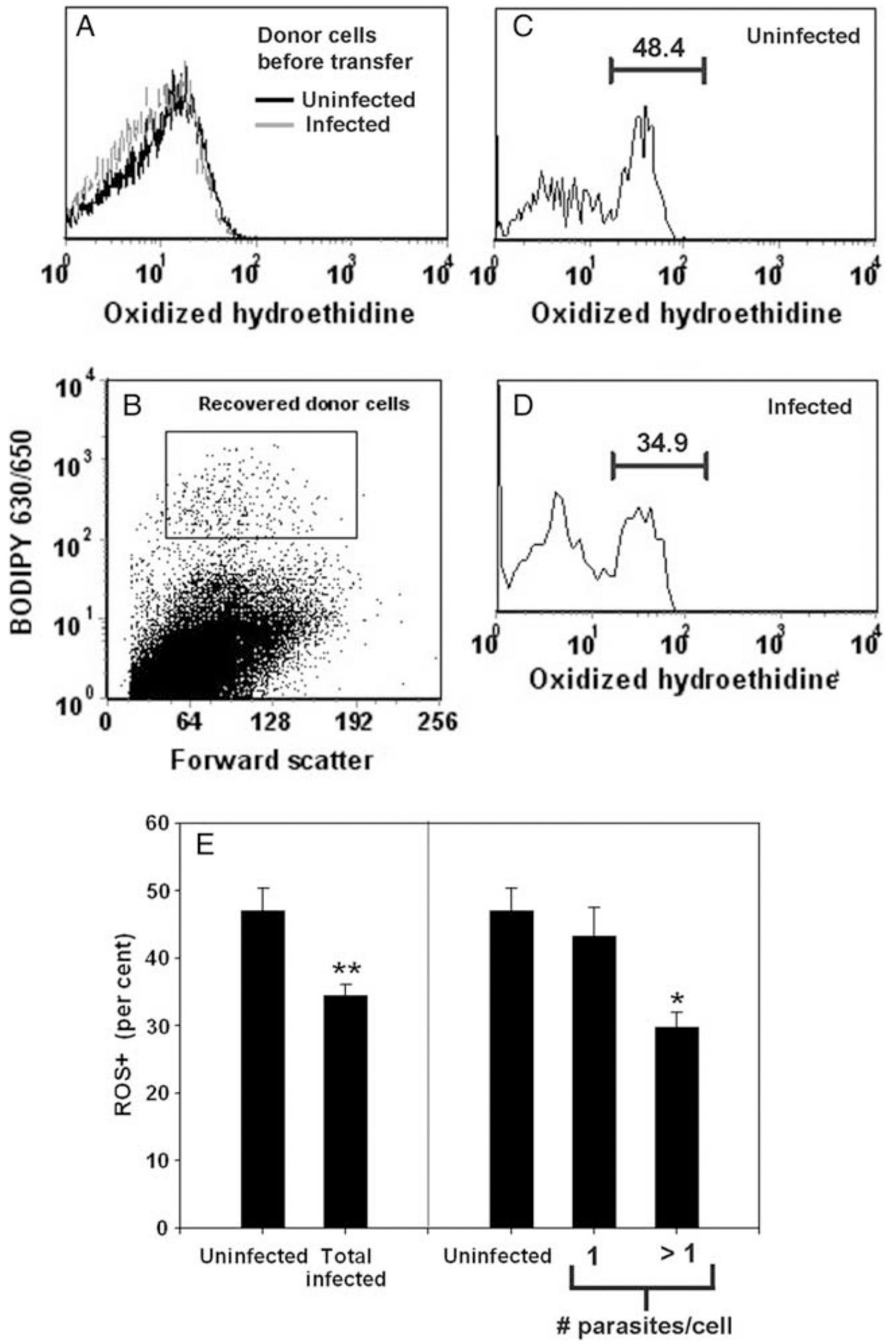

Fig. 8.

Prior infection of macrophages suppresses oxygen radical production in vivo. Vital dye-labeled macrophages from an infected culture (A) were recovered 90 min after transfer of 200,000 cells to infected mice (B) and assessed for ROS$^+$ fraction (C–E). Numbers in panels C and D represent the percentage of recovered donor cells (gated as shown in panel B) within the indicated ROS$^+$ region. Each bar in panel E represents the mean ± SEM of four mice. **$P < 0.01$ by paired *t*-test. *$P < 0.05$ by paired *t*-test. The data are representative of two similar experiments.